MICROBIOLOGICAL METHODS

A Label-Free Electrochemical Biosensor Based on a Reduced Graphene Oxide and Indole-5-Carboxylic Acid Nanocomposite for the Detection of *Klebsiella pneumoniae*

ZE ZHANG
Fudan University Pudong Medical Center, Shanghai Pudong Hospital, Department of Clinical Laboratory, 2800 Gongwei Rd, Huinan Town, Pudong, Shanghai 201399, China
HONG-WEI YU, GUANG-CAI WAN, JING-HUI JIANG, and NA WANG
The First Affiliated Hospital of the Harbin Medical University, No. 23 Youzheng St, Harbin, Heilongjiang Province 150001, China
ZHI-YONG LIU
The First Hospital of Suihua City, Intersection of Renhe St and Changjiang North Rd, Suihua, Heilongjiang Province 152000, China
DONG CHANG[1]
Fudan University Pudong Medical Center, Shanghai Pudong Hospital, Department of Clinical Laboratory, 2800 Gongwei Rd, Huinan Town, Pudong, Shanghai 201399, China
HONG-ZHI PAN
Harbin Medical University, Public Health School, No. 157 Baojian Rd, Nangang District, Harbin, Heilongjiang Province 150081, China

A label-free DNA hybridization electrochemical sensor for the detection of *Klebsiella pneumoniae* was developed, which could be helpful in the diagnosis of bacterial infections. Indole-5-carboxylic acid (ICA) and graphene oxide (GO) were electrodeposited on a glassy carbon electrode, and the resulting reduced GO (rGO)-ICA hybrid film served as a platform for immobilizing oligonucleotides on a single-stranded DNA (ssDNA) sequence. The conditions were optimized, with excellent electrochemical performance. A significant change was observed after hybridization of ssDNA with the target probe under optimum conditions. Hybridization with complementary, noncomplementary, one-base mismatched, and three-base mismatched DNA targets was studied effectively by differential pulse voltammetry. The proposed strategy could detect target DNA down to 3×10^{-11} M, with a linear range from 1×10^{-6} M to 1×10^{-10} M, showing high sensitivity. This electrochemical method is simple, free from indicator, and shows good selectivity. Hence, electrochemical biosensors are successfully demonstrated for the detection of *K. pneumoniae*.

Increasing concern regarding the microbiological safety of clinical diagnosis and water and environmental analyses has provided detection methods that are fast, sensitive, specific, and quantitative for high QA to prevent epidemics and infections (1–3). Among all pathogens, *Klebsiella pneumoniae* is a major cause of community and hospital-acquired infections (4). In the past decades, *K. pneumoniae* producing *K. pneumoniae* carbapenemase has spread globally (5). It is found naturally in the intestinal tracts of humans and warm-blooded animals and is characterized by diarrhea, urinary tract infections (6), bacteremia (7), and peritonitis (8) in immune-suppressed patients (9). The management of infections caused by *K. pneumoniae* has been complicated by the appearance of antimicrobial resistance, especially to the carbapenems (10). *K. pneumoniae* can produce carbapenemase and cause multidrug resistance. Early determination of this pathogen will have satisfactory clinical consequences for selecting an appropriate antibiotic regimen and for organizing and implementing effective surveillance and infection control measures (11).

At present, the methods of *K. pneumoniae* detection involve conventional techniques like traditional microbial culture–based tests (12), PCR (13, 14), and ELISA based on antibody–antigen interactions. The traditional microbial culture–based methods are sensitive and selective, but the main drawbacks of these techniques are long incubation times to obtain results and complex instrumentation requiring highly qualified technical staff. These methods cannot provide the detection results in real-time. To date, many other methods and techniques have been developed for the rapid detection of *K. pneumoniae*. However, these methods suffer from high costs, complex treatment procedures, easy contamination, and the inability to determine whether the detected pathogen was viable (15). To overcome the issues associated with the current diagnostic techniques, methods for the detection of *K. pneumoniae* in clinical diagnosis that are rapid, simple, inexpensive, and user-friendly must be developed. In addition, different bacterial genotypes could affect the clinical outcome of infectious disease. Therefore, the new methods need to offer selectivity to distinguish between closely related pathogenic and nonpathogenic microorganisms.

DNA biosensors, unlike other methods, respond to a minimal quantity of sample, yielding information on-line due to the

Received September 05, 2016. Accepted by AH October 28, 2016.
[1] Corresponding author's e-mail: dongchang1969@163.com
The authors greatly appreciate the support of this study from the National Natural Science Fund of China (grants 81273129 and 81573200).
DOI: 10.5740/jaoacint.16-0251

sensor and the signal transducer being in series. Among these, electrochemical techniques are increasingly being relied on due to advantages such as accuracy, simplicity, low cost, and fast response (16–18). They are used in the detection of DNA, with a view toward developing portable analytical devices. DNA biosensors present a simple, sensitive, and rapid platform for *K. pneumoniae* detection and could become a promising tool in clinical diagnosis.

In recent years, graphene and graphene oxide (GO) have emerged as fascinating materials. Their unique nanostructure and properties, such as high electrochemical activity, low cost, and large surface area, enable their potential application as biosensor-modified materials (19, 20). Much attention has been paid to these nanomaterials, including their synthesis and applications. Among these materials, reduced GO (rGO) is believed to be one of the best candidates due to its reasonably reduced number of functionalities, as well as effectively improving the electron transfer rate (21). Conducting polymers such as polypyrrole (22), polyaniline (23), polythiophene (24), and their various derivatives, have been widely used in recent years for developing various sensors. Conducting polymer–modified electrodes in genosensors are good alternatives for the immobilization of oligonucleotide (ODN) probes. Moreover, they provide an interface for the entrapment and attachment of ODN probes. Among conducting polymers, many functionalized polyindoles have been modified in the past due to their favorable properties. Poly(indole-5-carboxylic acid) (PICA), the derivative of polyindole, has shown good electrochemical performance and good stability (25, 26). The fabrication of an electrode modified with rGO and PICA was achieved by cyclic voltammetry (CV). No complicated immobilization or deleterious chemicals for signal enhancement were used.

In the present study, a *K. pneumoniae*-related conserved sequence as a probe was immobilized on an electrode. We describe the development of an electrochemical DNA biosensor for the rapid, specific, and sensitive detection of *K. pneumoniae*. This study illustrates some of the key working processes required for the future application of these biosensors in healthcare areas.

Experimental

Apparatus

Conventional three-electrode cell assemblies were used, with a modified glassy carbon electrode (GCE) as the working electrode and Pt wire serving as the auxiliary electrode (Incole Union Technology Co. Ltd, Tianjin, China). All potentials are referred to the silver chloride reference electrode (Ag/AgCl). Electrochemical characterizations, including CV and differential pulse voltammetry (DPV), were carried out on an electrochemical workstation (model CHI660D; Shanghai Chenhua Instruments Co. Ltd, China). All electrochemical measurements were carried out at room temperature. Scanning electron microscope (SEM) images were obtained using a Hitachi Fe-SEM S4800 instrument.

Reagents

GO was obtained from (JCNANO Co., Nanjing, China). Indole-5-carboxylic acid (ICA; 99%), 1-ethyl-3(3-dimethylaminopropyl) carbodiimide (EDC), and *N*-hydroxysuccinimide (NHS) were purchased from (Sigma, United States). Lithium perchlorate trihydrate ($LiClO_4 \cdot 3H_2O$, 99%) and acetonitrile (HPLC grade) were obtained from Fuchen Chemical Reagent Co. (Tianjin, China). All aqueous solutions were prepared using Milli-Q water (18.2 megohm cm). All reagents were of analytical grade and were used as supplied without further purification, unless otherwise stated.

All stock solutions were prepared in autoclaved water. All ODNs were dissolved in 10 mM Tris-HCl plus 1 mM EDTA (pH 8.00). The synthetic ODNs were purchased from (Sangon Biotech Co. Ltd, Shanghai, China), with the following sequences:

Immobilized probe: 5'HN_2-$(CH_2)_6$-5-TCT-GGA-CCG-CTG-GGA-GCT-GG-3'-GGA-CCG-CTG-GGA-GCT-GG-3′

Complementary target: 5′-CCA-GCT-CCC-AGC-GGT-CCT-GT-3′

One-base mismatch: 5′-CCA-GCT-CCC-ATC-GGT-CCT-GT-3′

Three-base mismatch: 5′-CTA-GCT-CCC-ATC-GGT-CAT-GT-3′

Noncomplementary: 5′-TTC-ATG-TTT-CAT-AAG-TTG-AG-3′

Electrochemical Polymerization

The electrochemical polymerization of ICA was carried out by CV under computer control at an appropriate potential of 1.2 V (Ag/AgCl). Before electropolymerization, the GCE was polished with 1.0 µm followed by 0.5 µm alumina slurry, and then washed with acetone, ethanol, and Milli-Q water.

We applied electropolymerization to deposit ICA and GO on the bare GCE. The polymerization solution contained 0.02 M ICA, 0.6 mg GO, and 0.1 M $LiClO_4 \cdot 3H_2O$ in 3 mL acetonitrile. The mixture was exfoliated by ultrasonication for 1 h to form a homogeneous colloidal dispersion. Under magnetic stirring, the CV reduction was carried out in the mixture, using a three-electrode system. The reduction was achieved after seven cycles because the thickness of the film was ideal. After polymerization, the rGO-ICA-GCE was scraped from the electrode surfaces and washed repeatedly in a solution of acetonitrile to remove unpolymerized monomers and electrolyte. The thickness of the film was controlled by the integrated charge passed through the cell during polymerization.

Probe Immobilization on GCE

The rGO-ICA-GCE was upturned, and 10 µL Tris-HCl buffer containing 5 mM EDC and 8 mM NHS was pipetted over the electrode surface for 1 h. Single-stranded DNA (ssDNA) solution (10 µL) was dropped on the electrode surface treated with EDC-NHS and kept for 2.5 h at room temperature. Next, the modified electrode was incubated below 10°C. The ssDNA probes were immobilized on the electrode surface through an amide bond between the NH_2 group of the ssDNA strand and the COOH group of ICA. The modified electrode was washed using sodium dodecyl sulfate (SDS; 3%) to remove the unattached DNA. The probe-immobilized electrodes were stored in the refrigerator at 4°C.

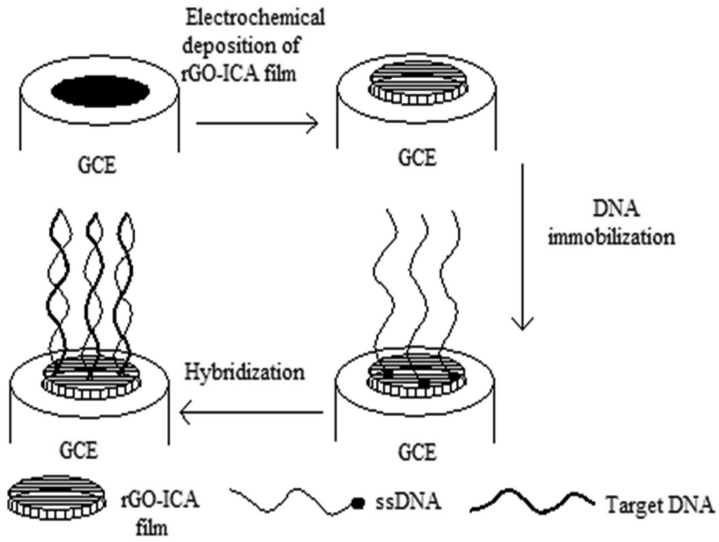

Figure 1. Schematic diagram showing the fabrication procedure of the rGO-ICA-modified DNA sensor for *K. pneumoniae* detection.

Hybridization

The electrode was upturned, and 10 µL target ODNs in Tris-HCl solution was pipetted over the electrode surface treated with probes for 30 min at 42°C. After hybridization, the electrode was washed using SDS to remove any nonhybridized ODNs.

The rGO-ICA-modified biosensor was fabricated as shown in Figure 1.

Results and Discussion

Characteristics of rGO-ICA Film

rGO was dispersed in ICA solution by ultrasonication for 1 h. The hydroxyl and amino functional groups of ICA combined with the hydroxyl and carboxyl groups of graphene, respectively, to form a well-dispersed rGO-ICA solution (27). Optimization of the electrodeposition conditions is important for developing an efficient biosensor. Major experimental variables affecting the electrodeposition are graphene concentration, electrodeposition time, and potential (28). The concentration of graphene was optimized within the range of 0–0.3 mg/mL. Figure 2 shows that although the resulting changes in peak current were not remarkable, they may have been caused by the differences in GCE substrate and the manual cutting operation. It was observed that the graphene concentration of 0.2 mg/mL was optimum for our study. At this concentration, the conductive nanocomposite–modified electrode showed the most stable signal. Beyond 0.2 mg/mL, we did not find evidence of any significant change in response.

Figure 3 shows SEM images of the rGO-ICA film. The film structure on the GCE was compact and flat. Microscopically, a spongelike matrix of polymer was constructed on the surface of the GCE (Figure 3a). This structure of rGO-ICA is beneficial to the stabilization of the dispersed biomaterials and the mass-transfer of electroactive species. Figure 3b shows the morphological changes, which resemble ordered arrangements of the nanoparticles. The microporous morphology indicates a large surface area, which makes it easy to immobilize ODN bound on the surface of electrode.

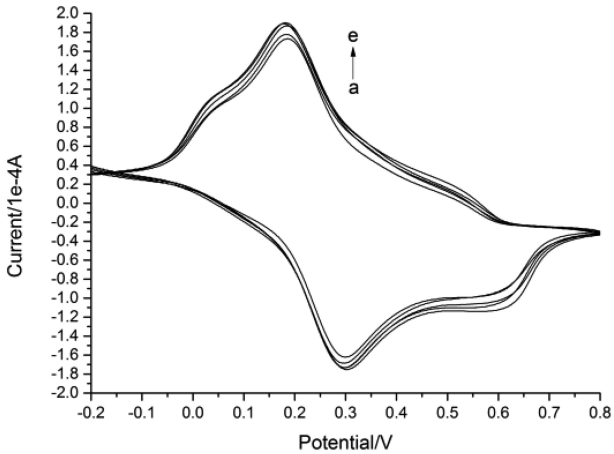

Figure 2. Cyclic voltammogram of electrodes showing the effect of graphene concentration on GCE electrodeposition. (a) 0 mg mL^{-1}; (b) 0.05 mg mL^{-1}; (c) 0.1 mg mL^{-1}; (d) 0.2 mg mL^{-1}; (e) 0.3 mg mL^{-1}.

Electrochemical Behaviors of Modified Electrodes, Immobilization of ODN, and Detection of Hybridization

The electrochemical behavior of the bare GCE and the rGO-ICA-GCE was evaluated by CV at a scan rate of 60 mV/s in 5 mM $K_4Fe(CN)_6/K_3Fe(CN)_6$ containing 0.1 M KCl. Figure 4 shows the electrochemical characteristics of the bare electrode, the ICA-GCE, and the rGO-ICA-GCE. Two obvious redox peaks at 300 and 180 mV were observed for the rGO-ICA-GCE compared to the bare electrode. This result indicates the formation of an electroactive polymer on the electrode surface. Figure 5 shows CV results of the rGO-ICA film at different scan rates between 40 and 140 mV/s. The linear dependence of the oxidation peak current on scan rate is presented in the inset of Figure 5 and demonstrates that the charge-transfer step controls the oxidation reaction rather than a diffusion step.

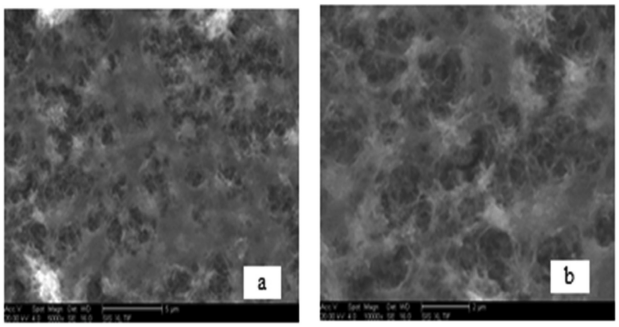

Figure 3. SEM micrographs of the rGO-ICA film deposited on the electrode surface using a polymerization solution containing 0.02 M ICA, 0.2 mg/mL GO, and 0.1 M $LiClO_4 \cdot 3H_2O$ monomer in acetonitrile. (a) Spongelike matrix of polymer constructed on the surface of the GCE. (b) Morphological changes resembling ordered arrangements of the nanoparticles.

The amino-substituted ODN probes were connected to the polymer by forming covalent bonds between amino and carboxyl groups, with the catalyst EDC-NHS.

Sensitivity and Selectivity

The sensitivity of the sensor was determined by incubating different amounts of complementary ODN with this electrochemical sensor. The calibration curves of the biosensor in Figure 6 (inset) show good linearity over the concentration rage from 1×10^{-6} to 1×10^{-10} M. The LOD of 3.3×10^{-11} M was achieved with sensors based on rGO-ICA using DPV.

To investigate selectivity of the sensor, several mismatched ODN targets were determined by measuring the response. Figure 7 shows the DPV results of the established sensor response for one- and three-mismatched sequences and for completely noncomplementary ODNs. When incubated with complementary ODNs, a significant decrease in the DPV curve was observed (Figure 7, curve e). The response to a noncomplementary ODN showed no significant differences to those initially obtained with the rGO-ICA electrode (Figure 7, curve b). After the incubation with one- and three-point mismatched strands, the changes of the DPV signal were 277.5 and 233.7 μA. The results show that the ICA-based DNA sensor has good selectivity.

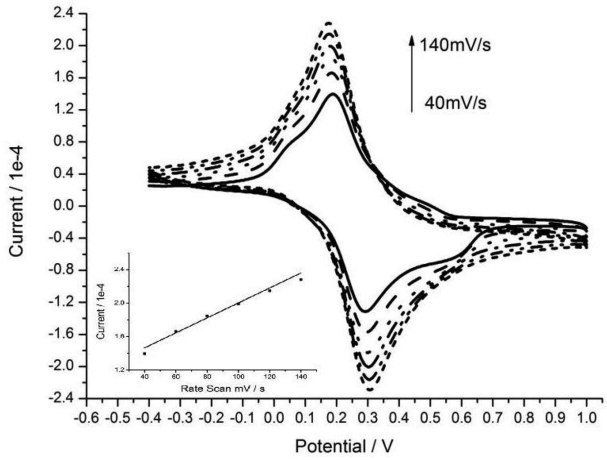

Figure 5. Cyclic voltammogram of rGO-ICA film in 5 mM $[K_4Fe(CN)_6/K_3Fe(CN)_6]$ containing 0.1 M KCl with different scan rates between 40 and 140 mV/s. (Inset: relationship of anodic current peaks as a function of scan rate for rGO-ICA film).

Stability of Biosensor

To investigate the stability of the sensor, the response of the sensor incubated with the ODN target was measured after 15 days (data not shown). It was observed that there was almost a 12.1% decrease in peak current response of the sensor. This result illustrates that the fabricated sensor retained 87.9% of its initial response after 15 days at 4°C.

Conclusions

In this work, a new functionalized rGO-ICA composite was synthesized and a label-free sensor for the detection of *K. pneumoniae* was developed using DPV as readout method. The

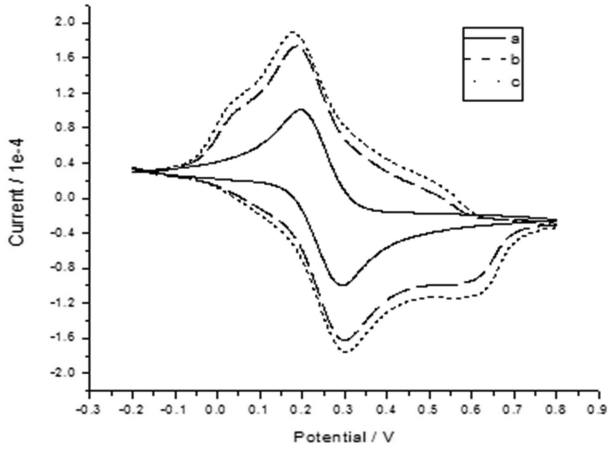

Figure 4. Cyclic voltammogram of the (a) bare electrode, (b) ICA-GCE, and (c) rGO-ICA-GCE in 5 mM $K_4Fe(CN)_6$ /$K_3Fe(CN)_6$ containing 0.1 M KCl. Scan rate: 60 mV/s.

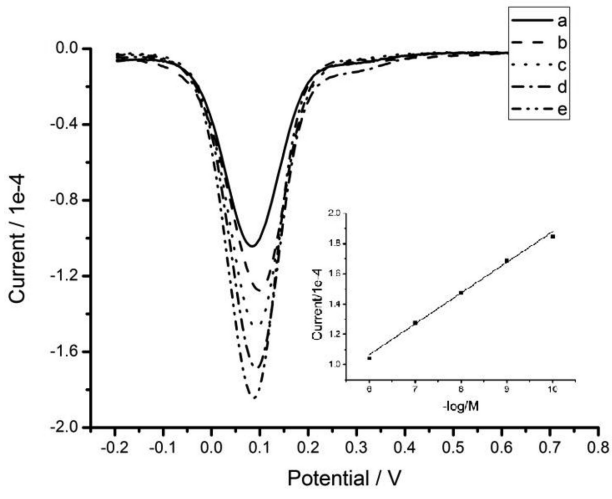

Figure 6. DPV peak curves of different concentrations of complementary strand. (a) 1×10^{-6} M; (b) 1×10^{-7} M; (c) 1×10^{-8} M; (d) 1×10^{-9} M; (e) 1×10^{-10} M. (Inset is the standard calibration curve of different concentrations of complementary sequence).

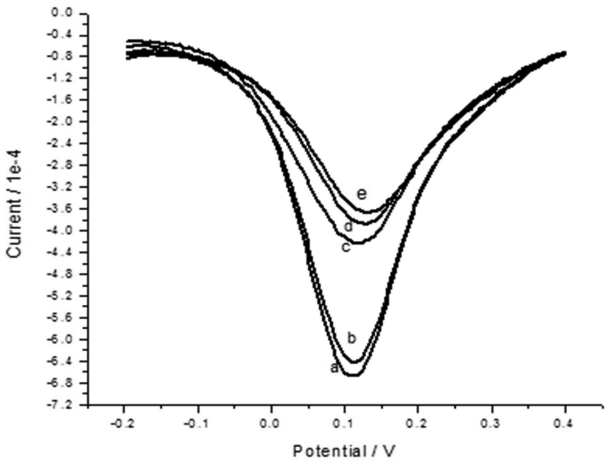

Figure 7. DPV peak curve changes of the sensor after hybridization with different ODN sequences (1×10^{-8} M). Curves: a, rGO-ICA probe; b, noncomplementary ODN; c, three-point mismatched ODN; d, one-point mismatched ODN; and e, complementary ODN. Scan rate: 60 mV/s.

K. pneumoniae-related 21-mer ODN sequence was gathered on the electrode, and hybridization with the ODN target was monitored via CV. The LOD of the sensor was 3.3×10^{-11} M. Our method could be helpful for further studies in clinical microbiology identification. This application of biosensors will speed up the translational process and can be used for *K. pneumoniae* detection.

Acknowledgments

This study was supported by grant 81273129 and 81573200 of the National Natural Science Fund of China and grant PWRI2016-04 of Outstanding Leaders Training Program of Pudong Health Bureau of Shanghai.

References

(1) Zhou, L., He, X., He, D., Wang, K., & Qin, D. (2011) *Clin. Dev. Immunol*. 2011, 193963. doi:10.1155/2011/193963

(2) Goh, Y.Y., Ho, B., & Ding, J.L. (2002) *Appl. Environ. Microbiol.* **68**, 6343–6352. doi:10.1128/AEM.68.12.6343-6352.2002

(3) Paniel, N., & Baudart, J. (2013) *Talanta* **115**, 133–142. doi:10.1016/j.talanta.2013.04.050

(4) Alicino, C., Giacobbe, D.R., Orsi, A., Tassinari, F., Trucchi, C., Sarteschi, G., Copello, F., Del Bono, V., Viscoli, C., & Icardi, G. (2015) *BMC Infect. Dis.* **15**, 415. doi:10.1186/s12879-015-1152-0

(5) van Duin, D., & Doi, Y. (2015) *J. Clin. Microbiol.* **53**, 3116–3117. doi:10.1128/JCM.01399-15

(6) Khatri, A., Nina Naeger Murphy, N., Wiest, P., Osborn, M., Garber, K., Hecker, M., Hurless, K., Rudin, S.D., Jacobs, M.R., Kalayjian, R.C., Salata, R.A., van Duin, D., Perez, F., Bonomo, R.A., Paterson, D.L., & Harris, P.N. (2015) *Antimicrob. Agents Chemother.* **59**, 4375–4378. doi:10.1128/AAC.00553-15

(7) Togawa, A., Toh, H., Onozawa, K., Yoshimura, M., Tokushiqe, C., Shimono, N., Takata, T., & Tamura, K. (2015) *J. Infect. Chemother.* **21**, 531–537. doi:10.1016/j.jiac.2015.04.004

(8) Kim, M.J., Song, K.H., Kim, N.H., Choe, P.G., Park, W.B., Bang, J.H., Kim, Es., Park, S.W., Kim, H.B., Lee, H.S., Oh, M.D., & Kim, N.J. (2014) *Hepatol. Int.* **8**, 582–587. doi:10.1007/s12072-014-9543-7

(9) Chang, L.W., Buising, K.L., Jeremiah, C.J., Cronin, K., Poy Lorenzo, Y.S., Howden, B.P., Kwong, J., Cocks, J., Blood, A., Greenough, J., & Waters, M.J. (2015) *Intern. Med. J.* **45**, 1037–1043. doi:10.1111/imj.12863

(10) Pitout, J.D., Nordmann, P., & Poirel, L. (2015) *Antimicrob. Agents Chemother.* **59**, 5873–5884. doi:10.1128/AAC.01019-15

(11) Voulgari, E., Poulou, A., Koumaki, V., & Tsakris, A. (2013) *Future Microbiol.* **8**, 27–39. doi:10.2217/fmb.12.130

(12) Lazcka, O., Del Campo, F.J., & Muñoz, F.X. (2007) *Biosens. Bioelectron.* **22**, 1205–1217. doi:10.1016/j.bios.2006.06.036

(13) Cuzon, G., Nass, T., Bogaerts, P., Glupczynski, Y., & Nordmann, P. (2013) *Diagn. Micr. Infec. Dis.* **76**, 502–505. doi:10.1016/j.diagmicrobio.2013.05.004

(14) Hindiyeh, M., Smollan, G., Grossman, Z., Ram, D., Robinov, J., Belausov, N., Ben-David, D., Tal, I., Davidson, Y., Shamiss, A., Mendelson, E., & Keller, N. (2011) *J. Clin. Microbiol*. **49**, 2480–2484. doi:10.1128/JCM.00149-11

(15) Vetrone, S.A., Huarng, M.C., & Alocilja, E.C. (2012) *Sensors* **12**, 10487–10499. doi:10.3390/s120810487

(16) Purushotham, M., Gupta, P., & Goyal, R.N. (2015) *Talanta* **143**, 328–334. doi:10.1016/j.talanta.2015.04.082

(17) Yang, T., Chen, H., Yang, R., Wang, X., Nan, F., & Jiao, K. (2015) *Colloids Surf., B* **133**, 24–31. doi:10.1016/j.colsurfb.2015.05.035

(18) Li, B., Pan, G., Avent, N.D., Lowry, R.B., Madgett, T.E., & Waines, P.L. (2015) *Biosens. Bioelectron.* **72**, 313–319. doi:10.1016/j.bios.2015.05.034

(19) Cui, X., Zhu, L., Wu, J., Hou, Y., Wang, P., Wang, Z., & Yang, M. (2015) *Biosens. Bioelectron.* **63**, 506–512. doi:10.1016/j.bios.2014.07.085

(20) Bai, H., Wang, C., Chen, J., Peng, J., & Cao, Q. (2015) *Biosens. Bioelectron.* **64**, 352–358. doi:10.1016/j.bios.2014.09.034

(21) Gao, W., Alemany, L.B., Ci, L., & Ajayan, P.M. (2009) *Nat. Chem.* **1**, 403–408. doi:10.1038/nchem.281

(22) Miodek, A., Mejri, N., Gomgnimbou, M., Sola, C., & Korri-Youssoufi, H.E.-D.N.A. (2015) *Anal. Chem.* **87**, 9257–9264. doi:10.1021/acs.analchem.5b01761

(23) Yang, T., Chen, H., Ge, T., Wang, J., Li, W., & Jiao, K. (2015) *Talanta* **144**, 1324–1328. doi:10.1016/j.talanta.2015.08.004

(24) Uygun, A. (2009) *Talanta* **79**, 194–198. doi:10.1016/j.talanta.2009.03.049

(25) Li, X., Xia, J., & Zhang, S. (2008) *Anal. Chim. Acta* **622**, 104–110. doi:10.1016/j.aca.2008.05.044

(26) Mohan, S., Nigam, P., Kundu, S., & Prakash, R. (2010) *Analyst (Cambridge, U. K.)* **135**, 2887–2893. doi:10.1039/c0an00258e

(27) Wan, Y., Lin, Z., Zhang, D., Wang, Y., & Hou, B. (2011) *Biosens. Bioelectron.* **26**, 1959–1964. doi:10.1016/j.bios.2010.08.008

(28) Qi, P., Wan, Y., & Zhang, D. (2013) *Biosens. Bioelectron.* **39**, 282–288. doi:10.1016/j.bios.2012.07.078